Generation of banded iron formations by internal dynamics and leaching of oceanic crust

Yifeng Wang[1]★, Huifang Xu[2], Enrique Merino[3] and Hiromi Konishi[2]

The chemical signatures and mineralogy of banded iron formations have the potential to provide information about the ocean environment on early Earth[1-7]. Their formation requires iron- and silicon-rich fluids, but the mechanisms by which the alternating layers of Si- and Fe-rich rock formed remain controversial[8-11]. Here we use thermodynamic calculations to show that Fe- and Si-rich fluids can be generated by hydrothermal leaching of low-Al oceanic crustal rocks such as komatiites. We find that positive feedbacks occur among the chemical reactions when hydrothermal fluids mix with ambient sea water. These feedbacks lead to alternating precipitation of Fe and Si minerals, owing to the formation of complexes between Fe(II) and silicic acid. We suggest that the small-scale (<1 cm) banding was produced by internal dynamics of the geochemical system, rather than any external forcing. As the Archaean eon progressed, the oceanic crust produced was rich in Al[12]. When Al-rich crust undergoes hydrothermal alteration, Fe is locked in Al–Fe silicate minerals. This results in iron-depleted hydrothermal fluids, and thus prevents the deposition of Fe-rich minerals. We therefore conclude that the widespread cessation of banded iron formation deposition 1.7 billion years ago reflects the changing composition of the oceanic crust.

Banded iron formations (BIFs) are massive chemical deposits composed of alternating layers of chert and iron-rich minerals (such as haematite, magnetite and siderite), with three scales of bandings—microbands (≤1 mm), mesobands (~1 mm–10 cm) and macrobands (≥1 m; refs 1–3). BIFs have been extensively studied as an indicator for chemical and biological evolution of the early Earth[4,5]. Their abundance in the Archaean/early Proterozoic era and their absence[6] thereafter suggest that chemical conditions and iron transport pathways on the early Earth surface were different from those after 1.7 billion years (Gyr) ago[7]. BIF bandings have been attributed to seasonal temperature variations[8,9], microbially catalysed Fe(III) (hydr)oxide precipitation triggered by ocean temperature fluctuations[10], episodic fluid mixing[3] and deposition by density currents[11]. However, surface temperature variations cannot be responsible for the formation of BIFs in deep-water environments[3], and in any case, such seasonal surface temperature variations were probably not significant in the warm Archaean atmosphere[13]. Low organic carbon contents in BIFs suggest that microbial activity might not have a significant role in BIF precipitation[2].

A reasonable BIF formation model must address three key issues. It must account for the generation of large volumes of water containing roughly comparable, and high, contents of dissolved SiO₂ and Fe(II). It must also provide a credible mechanism for oscillatory precipitation of iron and silica minerals. Finally, it must account for both the worldwide abundance of BIFs in the Archaean/early Proterozoic era and their disappearance after

1.7 Gyr ago and their occurrence in both shallow- and deep-water environments. Here we present a new model that successfully addresses all of these issues.

Our model assumes that a BIF forms by mixing of a discharged submarine hydrothermal fluid (or plume) with its ambient sea water[2,3] (Fig. 1). The fluid acquires dissolved SiO_2 and Fe(II) through seawater circulation and leaching in the oceanic crust. Fe^{2+} is predicted to form a strong complex with silicic acid, $Fe^{2+} + H_3SiO_4^- = FeH_3SiO_4^+$, with $\log K = 10^{4.8}$ (Fig. 2). Thus, silica and Fe(II) can be leached out simultaneously from the oceanic crust in high and comparable amounts. In contrast, owing to their low stability constants with silicic acid (Fig. 2), Ca and Mg would be differentially left behind in the crust during leaching. This may explain the rarity of Archaean dolomite-limestone deposition[14] despite high Archaean atmospheric CO_2 concentrations[15]. The mobilization of transition metals (such as Zn and Pb) and the formation of ore deposits of these metals were still possible however during that time period[6].

Now the question is: under what conditions can the circulating fluid acquire roughly equal and high concentrations of dissolved SiO_2 and Fe(II)? Our thermodynamic calculations show that such a fluid can be generated only from low-Al oceanic rocks such as komatiites (Fig. 3a), but not from modern oceanic basalts (Fig. 3b), which have a high Al content. The concentration of dissolved Fe(II) in a fluid that has reacted with such basalts is orders of magnitude lower than that of dissolved SiO_2 over the whole range of solid/water ratios (Fig. 3b). This low concentration results from the fact that Fe(II) is locked up by abundant Fe(II)–Al chlorite formed during the hydrothermal alteration. In contrast, the alteration of komatiites results mainly in serpentinization; the scarcity of Al keeps chlorites from forming and thus leaves the Fe free to be leached out. Given the stoichiometry of chlorite $[(Fe,Mg)_5Al_2Si_3O_{10}(OH)_8]$, a necessary condition for the generation of Fe–Si-rich hydrothermal plumes is that the molar ratio of Al/(Fe + Mg) in oceanic rocks must be <2:5, a condition satisfied by komatiites or komatiitic basalts. A similar argument applies to Mg/Si ratios. Too high Mg contents in oceanic crust could lock up considerable silica as serpentine $[Mg_3(Si_2O_5)(OH)_4]$. The predicted alkaline nature of ancient hydrothermal systems (Fig. 3a,b) is supported by the recent discovery of the Lost City hydrothermal field developed in ultramafic rocks, where the pH ranges from 9 to 11 (ref. 16).

Systematic compositional analyses of komatiites and the related melting experiments reveal general trends of early oceanic crust evolution: (1) Mg contents were high before 3.5 Gyr ago and then decreased with time; (2) Al, Ca and Na increased as Mg decreased; (3) Si and Fe remained roughly constant[12]. Our calculations thus suggest that the presence of low-Al ultramafic rocks (for example, komatiitic rocks) in the early oceanic crust were probably the

[1]Sandia National Laboratories, PO Box 5800, Albuquerque, New Mexico 87185, USA, [2]Department of Geology and Geophysics and NASA Astrobiology Institute, University of Wisconsin, Madison, Wisconsin 53706, USA, [3]Department of Geological Sciences, Indiana University, Bloomington, Indiana 47405, USA. *e-mail: ywang@sandia.gov.
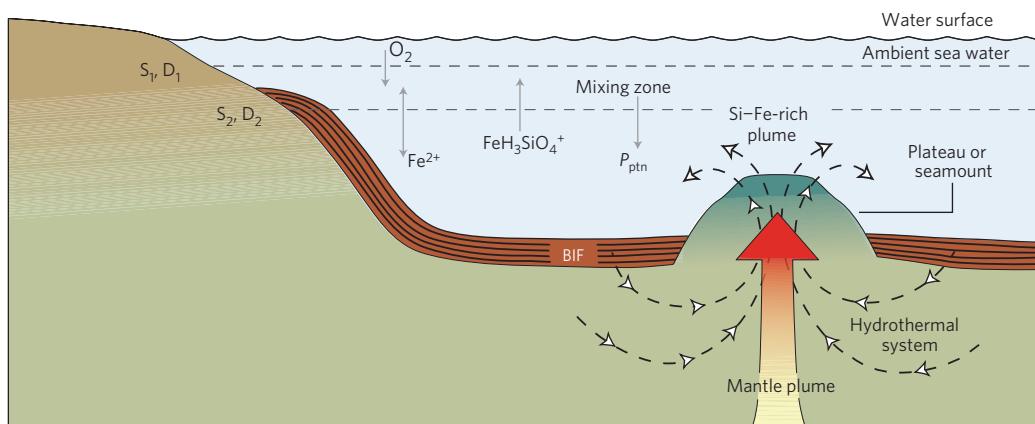
Figure 1 | Precipitation of BIFs from a hydrothermal system. The ambient sea water could be either oxic or anoxic (only oxic is shown here). Komatiitic rocks formed as a part of plateau or seamount above a deep mantle plume. Periodic precipitation of iron oxide and silica was induced through a self-organization mechanism. P_{ptn}: mineral precipitation; S_1, D_1: the area of the upper surface of the mixing zone and the corresponding mass exchange coefficient for mixing respectively; S_2, D_2: the area of the lower surface of the mixing zone and the corresponding mass exchange coefficient for mixing, respectively.
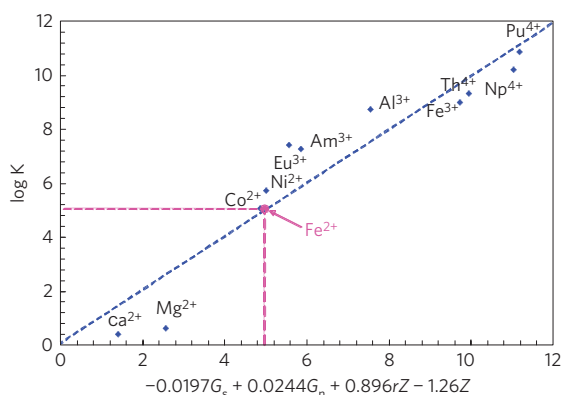
Figure 2 | Prediction of stability constant of $FeH_3SiO_4^+$ using a linear free-energy correlation. Fe^{2+} is predicted to form a strong complex with silicic acid. This complexation has an important role in controlling dissolved SiO_2 and Fe(II) in a geologic fluid leaching through an oceanic crust. Data for stability constants are taken from ref. 27. G_s and G_n are the solvation energy and the non-solvation energy of a cation respectively; r and Z are the ionic radius and the charge of a cation, respectively[28,29].

reason for both the formation of BIFs and their abundance in the Archaean/early Proterozoic era. This is consistent with the findings that the ages of komatiites are correlated strongly, at the 99% confidence level, with the ages of BIFs (ref. 17) and that the Ni content of BIFs is correlated with the eruption of ultramafic rocks[5]. High heat flux from the Precambrian upper mantle[14] would have further enhanced hydrothermal leaching and BIF formation[18]. After ~1.7 Gyr ago, increasing Al in the oceanic crust, owing to the disappearance of komatiites following from the abating of deep mantle plume activity, promoted growth of sufficient Fe-trapping aluminous chlorite, thus hindering the generation of Si–Fe-rich hydrothermal fluids for BIF formation. Similarly, the scarcity of BIF precipitation before ~3.5 Gyr ago may be due to too high Mg contents in Hadean and early Archaean oceanic crust that would have inhibited Si leaching by the precipitation of serpentine.

The thermodynamic calculations also show that the sulphate in the leaching sea water could be reduced and precipitated as Fe sulphides during hydrothermal alteration. Owing to the great concentration disparity between sulphate in the sea water and iron in a typical oceanic rock, however, sulphide precipitation

accounts for only a very small fraction of iron precipitated during leaching. This result contradicts the existing hypothesis that rising oceanic sulphur levels may have caused the disappearance of BIFs after ~1.7 Gyr ago[19].

For BIF formation, our model requires that only some portion of the bulk oceanic crust was komatiitic. As ocean crust composed of komatiites tended to form a part of oceanic plateaux/seamounts[17], Fe and Si leached from these rocks could be transported away and deposited on the surrounding sea floor (Fig. 1). BIFs thus did not have to precipitate directly on their source rocks.
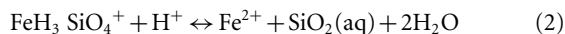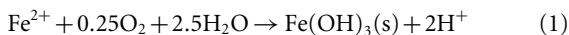
A second condition for BIF formation is that the leaching should be carried out by moderately alkaline (pH = 7.2–9.0) fluids, as very alkaline water would dissolve much more silica than Fe(II), and acid water would dissolve much more Fe(II) than silica (Fig. 3c). This pH range is constrained by assuming that the leaching fluid is equilibrated with $Fe(OH)_2(s)$ and SiO_2(amorphous). The formation of Fe-rich brucite-like mineral phases was observed for olivine serpentinization[20]. Together with Al enrichment, an increase in Na and Ca contents in the oceanic crust tends to push the pH of hydrothermal fluids to the higher end, outside the optimal pH range, thus not favouring BIF formation (Fig. 3c). Similarly, if the leached rock initially contains sufficient Fe sulphides, as the modern oceanic crust does, the oxidation of these sulphides by the leaching sea water could push the pH of hydrothermal fluids to a low value outside the optimal range, thus again not favouring BIF formation.

When a Fe–Si-rich fluid accumulates at the bottom of a sedimentary basin, it starts to mix with either oxic or anoxic ambient sea water. Let us consider the case of mixing with oxygenated sea water (Fig. 1). In the mixing zone, O_2 is supplied from above and Fe(II) and SiO_2(aq) from below. Within this zone, non-equilibrium chemical conditions prevail—a necessary condition for the emergence of chemical oscillations. The concept of self-organized chemical oscillations has been used to explain the genesis of various repetitive textures in geologic formations without invoking external periodic forces[21]. A self-organized chemical oscillation requires that one or more positive feedbacks operate among the chemical and physical processes involved in a system[22]. Within the mixing zone, three positive feedbacks are possible: (1) release of H^+ from Fe^{2+} precipitation, which causes Fe^{2+} dissociation from silicic acid and thus further promotes Fe^{2+} precipitation; (2) release of certain cations from silica precipitation, which further promotes silica precipitation[21]; (3) oxidation of Fe(II) catalysed by its product[23]. To illustrate the concept, here we focus
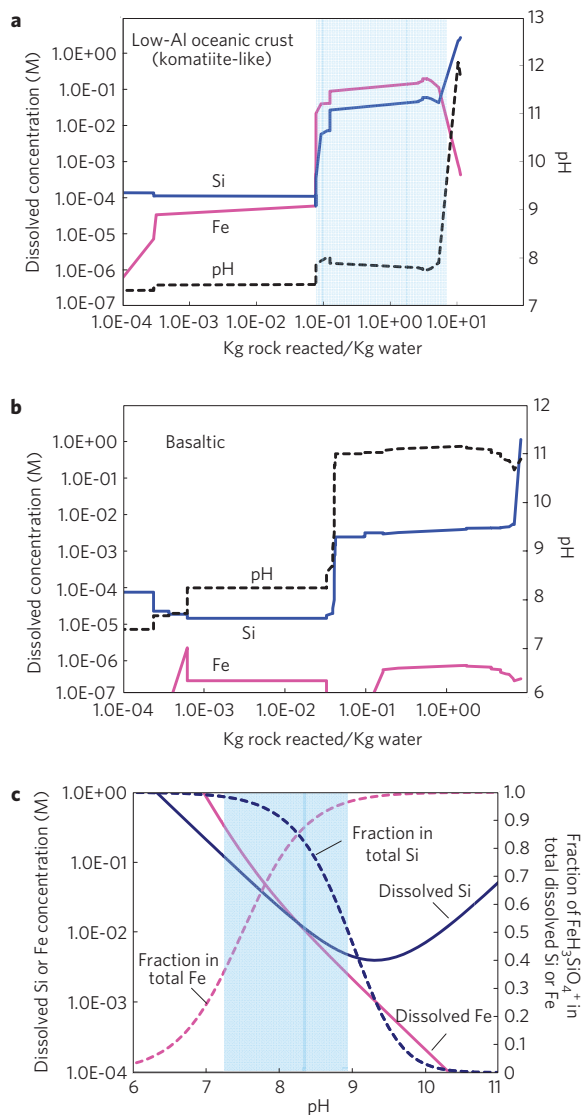
Figure 3 | Dissolved Si and Fe concentrations in a hydrothermal plume. The shaded regions represent the ranges of rock/water ratios for leaching out roughly equal concentrations of Si and Fe. The fractions of $FeH_3SiO_4^+$ in total dissolved Fe or Si are indicated by the dashed lines. The actual range of solid/water ratio of a hydrothermal system is determined by the velocity of water percolation, the length of flow path and the rate of rock dissolution.

only on the first feedback involving the following reactions:

$$Fe^{2+} + 0.25O_2 + 2.5H_2O \rightarrow Fe(OH)_3(s) + 2H^+ \quad (1)$$

$$FeH_3SiO_4^+ + H^+ \leftrightarrow Fe^{2+} + SiO_2(aq) + 2H_2O \quad (2)$$

Assume that the pH of the fluid is ~8.2, for which $FeH_3SiO_4^+$ is the dominant aqueous species of dissolved Fe(II) and SiO₂ (Fig. 3c). H^+ ions released by reaction (1) drive reaction (2). One Fe^{2+} precipitated by reaction (1) causes two Fe^{2+} ions dissociated in reaction (2), which increases the Fe^{2+} concentration and further accelerates reaction (1). Assuming that reaction equation (2) remains instantaneously in equilibrium, we can combine the two reactions into:

$$2FeH_3SiO_4^+ + Fe^{2+} + 0.25O_2 \rightarrow Fe(OH)_3 + 2Fe^{2+}$$
$$+ 2SiO_2(aq) + 1.5H_2O$$
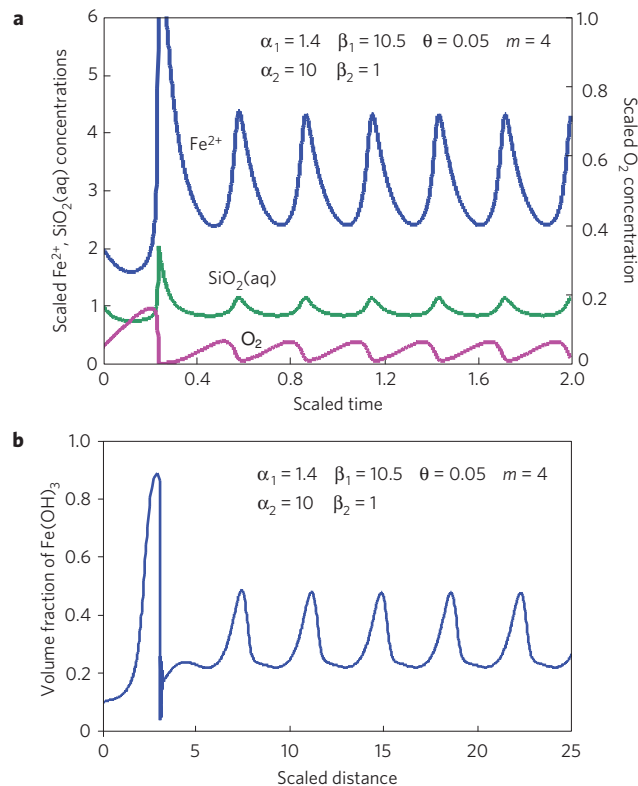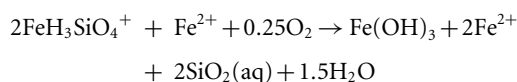
Figure 4 | Self-organized oscillatory precipitation of BIF in a mixing zone of a Si–Fe-rich hydrothermal fluid with the ambient sea water. The dissolved concentrations are scaled to their boundary values. $\alpha_1 = VR_1(X^0, Y^0)/(S_1D_1X^0)$, $\beta_1 = X^0/Y^0$, $\alpha_2 = VR_2(Z^0)/(S_1D_1Z^0)$, $\beta_1 = X^0/Z^0$ and $\theta = S_1D_1/(S_2D_2)$.

This overall reaction is driven by reaction (1). Being far-from-equilibrium, the rate of this reaction can be described by[24]:

$$R_1 = k_1[O_2][Fe^{2+}]^m$$

where m is a positive constant and the brackets indicate concentrations. Similarly, the rate of silica precipitation $SiO_2(aq) \rightarrow SiO_2(am)$ is described by:

$$R_2 = k_2[SiO_2(aq)]$$

With notations of $X \equiv [O_2]$, $Y \equiv [Fe^{2+}]$ and $Z \equiv [SiO_2(aq)]$, the precipitation of a BIF in the mixing zone can be described by:

$$V\frac{dX}{dt} = S_1D_1(X^0 - X) - 0.25VR_1 \quad (3)$$

$$V\frac{dY}{dt} = S_2D_2(Y^0 - Y) + VR_1 \quad (4)$$

$$V\frac{dZ}{dt} = S_2D_2(Z^0 - Z) + 2VR_1 - VR_2 \quad (5)$$

where V is the volume of the mixing zone. S_i and D_i are defined in Fig. 1. The superscript '0' indicates the concentrations outside the mixing zone. A scaling analysis shows that the concentration of $FeH_3SiO_4^+$ remains roughly constant as the concentrations of O_2, Fe^{2+} and $SiO_2(aq)$ vary, because $FeH_3SiO_4^+$ has a much higher boundary concentration than the others.

Numerical solutions of equations (3)–(5) show that periodic precipitation of iron hydroxide and silica emerges in the mixing zone even with constant boundary conditions (Fig. 4). This self-organization mechanism works equally well for the precipitation of siderite BIFs, because the positive feedback between reactions (1) and (2) still operates if O_2 is replaced with CO_2. Furthermore, this feedback also operates well if reaction (1) is replaced with an anoxygenic Fe(II)-oxidizing microbial reaction[10]:

$$Fe^{2+} + 0.25HCO_3 + 2.5H_2O \rightarrow Fe(OH)_3 + 0.25CH_2O + 1.75H^+$$
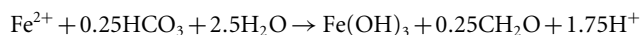
The typical thickness of each band (L_b) is calculated by:

$$L_b \approx L_{mix}\overline{C}V^m$$

where L_{mix} is the thickness of the mixing zone (1–10 m), $\overline{C}$ is a typical concentration of dissolved O_2 or CO_2 ($\sim 10^{-4}$–10^{-2}M) and V^m is a typical formula volume for oxides ($\sim 20\,cm^3\,mol^{-1}$). The thickness of a band is estimated to range from $\sim 10\,\mu m$ to $\sim 1\,cm$, in good agreement with field observations (see Supplementary Information). Given high atmospheric CO_2 concentrations in the Archaean era, the dissolved concentration of CO_2 in sea water could be high—higher than the dissolved O_2 concentration. Siderite BIFs are thus predicted to have larger band spacings than iron oxide BIFs. Large-scale bandings ($> 10\,cm$) were probably formed by multiple hydrothermal events.

Under certain conditions, some part of a Fe–Si-rich plume might not react with either O_2 or CO_2. The Fe(II)–silicic complexes in that part of the plume might form colloids and gradually coalesce into granules (grains). This is supported by the rare occurrence of greenalite iron formations (see Supplementary Information), presumably formed by[2,25]:

$$3Fe(II)SiO_3 \cdot H_2O \rightarrow Fe(II)_3Si_2O_5(OH)_4 \text{ (greenalite)} + SiO_2 \text{ (chert)} + H_2O$$
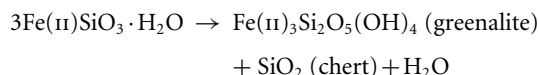
The occurrence of greenalite iron formation is thus an indicator for the involvement of Fe(II)–silicic complexes in BIF formation.

Methods

The thermodynamic calculations were carried out using computer code EQ3/6 in its 'fluid-centred' mode[26]. The thermodynamic database associated with the code was revised to incorporate metal–silicic acid complexation constants constrained from a linear free-energy correlation (Fig. 2). As a result of insufficient thermodynamic data, all calculations were carried out for the temperature of 25 °C. Various chemical compositions of komatiites and basalts were used in the calculations. Figure 3 shows the results for the following hypothetical rock compositions (wt%): komatiite—SiO_2 (55.0), Al_2O_3 (2.2), FeO (20.0), MgO (22.0), CaO (0.1), Na_2O (0.1) and K_2O (0.01); basalt[14]—SiO_2 (49.8), Al_2O_3 (16.0), FeO (9.0), MgO (7.5), CaO (11.2), Na_2O (2.75) and K_2O (0.14).

References

1. Trendall, A. F. The significance of iron-formation in the Precambrian stratigraphic record. *3 Int. Assoc. Sedimentol. Spec. Publ.* **33,** 33–66 (2002).
2. Klein, C. Some Precambrian banded iron-formations (BIFs) from around the world: Their age, geologic setting, mineralogy, metamorphism, geochemistry, and origin. *Am. Mineral.* **90,** 1473–1499 (2005).
3. Ohmoto, H. *et al.* Chemical and biological evolution of early Earth: Constraints from banded iron-formations. *Geol. Soc. Am. Memoir* **198,** 291–331 (2006).
4. Canfield, D. E. The Early History of atmospheric oxygen: Homage to Robert M. Garrels. *Annu. Rev. Earth. Planet. Sci.* **33,** 1–36 (2005).
5. Konhauser, K. O. *et al.* Oceanic nickel depletion and methanogen famine before the great oxidation event. *Nature* **458,** 750–754 (2009).
6. Meyer, C. Ore metals through geologic history. *Science* **227,** 1421–1428 (1985).
7. Johnson, C. M., Beard, B. L., Klein, C., Beukes, N. J. & Roden, E. E. Iron isotopes constrain biologic and abiologic processes in banded iron formation genesis. *Geochim. Cosmochim. Acta* **72,** 151–169 (2008).
8. Drever, J. I. Geochemical model for the origin of Precambrian banded iron formations. *Geol. Soc. Am. Bull.* **85,** 1099–1106 (1974).
9. Garrels, R. M. A model for the deposition of the microbanded Precambrian iron formations. *Am. J. Sci.* **287,** 81–106 (1987).
10. Posth, N. R., Hegler, F., Konhauser, K. O. & Kappler, A. Alternating Si and Fe deposition caused by temperature fluctuations in Precambrian oceans. *Nature Geosci.* **1,** 703–708 (2008).
11. Krapez, B., Barley, M. E. & Pickard, A. L. Hydrothermal and resedimented origins of the precursor sediments to banded iron-formation: Sedimentological evidence from the Early Palaeoproterozoic Brockman Supersequence of Western Australia. *Sedimentology* **50,** 979–1011 (2003).
12. Arndt, N. T., Lesher, C. M. & Barnes, S. J. *Komatiite* (Cambridge Univ. Press, 2008).
13. Kasting, J. F. & Howard, M. T. Atmospheric composition and climate on the early Earth. *Phil. Trans. R. Soc. B* **361,** 1733–1742 (2006).
14. Condie, K. C. *Plate Tectonics & Crustal Evolution* 3rd edn (Pergamon, 1989).
15. Bebout, B. M. *et al.* Methane production by microbial mats under low sulphate concentrations. *Geobiology* **2,** 87–96 (2004).
16. Martin, W., Baross, J., Kelley, D. & Russell, M. J. Hydrothermal vents and the origin of life. *Nature Rev. Microbiol.* **29,** 1–10 (2008).
17. Isley, A. E. & Abbott, D. H. Plume-related mafic volcanism and the depeosition of banded iron formation. *J. Geophys. Res.* **44,** 15461–15477 (1999).
18. Isley, A. E. Hydrothermal plumes and delivery of iron to banded iron formation. *J. Geol.* **103,** 169–185 (1995).
19. Poulton, S. W., Fralick, P. W. & Canfield, D. E. The transition to sulphidic ocean ~1.84 billion years ago. *Nature* **431,** 173–177 (2004).
20. Beard, J. S. *Geological Society of America Meeting* (Houston, 2008).
21. Merino, E. & Wang, Y. in *Non-Equilibrium Processes and Dissipative Structures in Geoscience, Self-Organization Yearbook* Vol. 11 (eds Krug, H.-J. & Kruhl, J. H.) 13–45 (Duncker & Humblot, 2001).
22. Nicolis, G. & Prigogine, I. *Self-Organization in Non-Equilibrium Systems* (Wiley, 1977).
23. Sung, W. & Morgan, J. J. Kinetics and product of ferrous iron oxygenation in aqueous systems. *Environ. Sci. Technol.* **14,** 561–568 (1980).
24. Millero, F. J., Sotolongo, S. & Izaguirre, M. The oxidation kinetics of Fe(II) in seawater. *Geochim. Cosmochim. Acta* **51,** 793–801 (1987).
25. Simonson, B. M. Origin and evolution of large Precambrian iron formations. *Geol. Soc. Am. Spec. Paper* **370,** 231–244 (2003).
26. Wolery, T. J. & Jarek, R. L. *EQ3/6, A Software Package for Geochemical Modeling of Aqueous Systems* Vol. 8.0 (Sandia National Laboratories, 2003).
27. Thakur, P., Singh, D. K. & Choppin, G. R. Polymerization study of o-Si(OH)$_4$ and complexation with Am(III), Eu(III) and Cm(III). *Inorg. Chim. Acta* **360,** 3705–3711 (2007).
28. Wang, Y. & Xu, H. Prediction of trace metal partitioning between minerals and aqueous solutions: A linear free energy correlation approach. *Geochim. Cosmochim. Acta* **65,** 1529–1543 (2001).
29. Xu, H., Wang, Y. & Barton, L. L. Application of a linear free energy relationship to crystalline solids of MO_2 and $M(OH)_4$ phases. *J. Nucl. Mater.* **273,** 343–346 (1999).

Author contributions

Y.W. and H.X. formulated the model and Y.W. drafted the paper; E.M. contributed to conceptual model development and part of the writing; H.X. and H.K. provided the Supplementary Information.

Additional information